Reflective walk based on lifted leg control and vision-cued swaying control

Takahiro Miyashita, Koh Hosoda, and Minoru Asada
Dept. of Adaptive Machine Systems
Graduate School of Engineering, Osaka University
Yamadaoka 2-1, Suita, Osaka, Japan 565-0871

Abstract

This paper presents a reflective walk based on lifted leg control and vision-cued swaying control [1] for a vision guided quadruped robot. The lifted leg control generates a reflective gait which consists of three steps: 1) select a leg to lift so as to increase the body stability, 2) shift (lift up, move, and down) one of other legs to enable the selected leg lifted, and 3) shift the selected leg. During these steps, vision-cued swaying control generates a swaying motion of the robot so that it can stabilize the visual target at the desired position in the image. Combining the reflective gait and the swaying, the robot attempts at tracking the visual target, and as a result a reflective walk emerges. The validity of the method is shown by a preliminary experiment, and future work is given.

1 Introduction

Legged locomotion has been attracting many researchers not only as a method of navigation on rough terrains but also due to its biological interests in realizing artificial systems similar to legged animals owing to many degrees of freedom. Most existing methods have considered kinematics and/or dynamics of the legged robots, calculated desired trajectories of the joints, and applied internal sensory feedback so that the robot can control leg motions to follow the trajectories [2]. Therefore, these robots seem difficult to adapt themselves to changes in their environments. To cope with these changes, reflective motions based on external sensors such as vision, tactile, and force sensors seem necessary as we can see in many living systems.

There are some work to realize reflective walks for human-operated walking control [3, 4]. Salmi and Halme [3] built a motion planner to the six-legged walking robot, "MECANT", and realized a reflective walk. Their method is, however, difficult to apply to quadruped robots directly because it is difficult to keep static stability. Adachi et al. [4] realized a reflective gait for the quadruped robot by a body propulsive action and recovery ones. However, they need a strong assumption on horizontal, planar terrain in order to realize stable lift-down actions. Therefore, their method seems difficult to apply to non-horizontal, planar terrain.

In this paper, we propose a reflective walk based on lifted leg control and vision-cued swaying control [1] for vision guided quadruped robot. The lifted leg control generates a reflective gait which consists of three steps: 1) select a leg to be lifted so as to increase the body stability, 2) shift (lift up, move, and down) one of other legs to enable the selected leg lifted, and 3) shift the selected leg. During these steps, vision-cued swaying control generates a swaying motion of the robot so that it can stabilize the visual target at the desired position in the image. Combining the reflective gait and the swaying, the robot attempts at tracking the visual target coping with changes in body stability, and as a result a reflective walk emerges on rough terrain.

The rest of this article is structured as follows. In the next section, we explain our method for reflective walking. Then, we show a preliminary experimental results in a real environment to verify the proposed method. Finally, the future work is given.

2 A Legged robot

We use a following quadruped robot as a legged robot (see Figure 1) which has:

- four legs, each of which has three degrees of freedom,
- four force sensors attached to each foot,
- an uncalibrated TV camera, and

- twelve joint angle sensors.

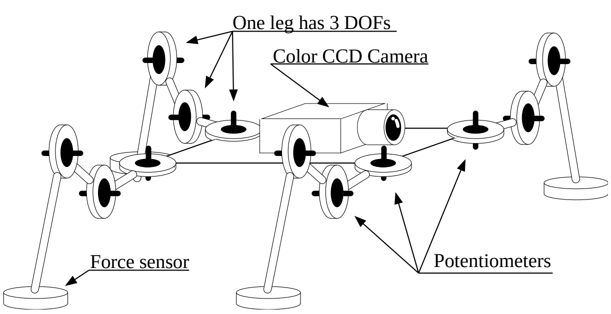

Figure 1: A legged robot

3 Vision-cued swaying control [1]

We apply the adaptive visual servoing [5] to the legged robot in order to track visual targets. As a result, the robot realizes swaying. We give a brief explanation of the swaying controller.

Let Σ_R, ${}^R\boldsymbol{p}$, ${}^R\boldsymbol{r}_i$ and $\boldsymbol{l}$ denote a robot coordinate frame fixed to the robot body, a position vector of a camera attached to the robot with respect to Σ_R, the i-th foot position vector w. r. t. Σ_R and a stance vector consists of distances between feet, respectively. Defining ${}^R\boldsymbol{r}$ by

$$ {}^R\boldsymbol{r} \triangleq \left[{}^R\boldsymbol{r}_1^T \, {}^R\boldsymbol{r}_2^T \cdots {}^R\boldsymbol{r}_n^T \right]^T \quad , \tag{1} $$

we can obtain two velocity relations,

$$ \dot{\boldsymbol{l}} = \boldsymbol{J}_{lr} \, {}^R\dot{\boldsymbol{r}} \quad , \tag{2} $$

$$ {}^R\dot{\boldsymbol{p}} = \boldsymbol{J}_{pr} \, {}^R\dot{\boldsymbol{r}} \quad , \tag{3} $$

where $\boldsymbol{J}_{lr} = \partial \boldsymbol{l} / \partial {}^R\boldsymbol{r}^T$ and $\boldsymbol{J}_{pr} = \partial \boldsymbol{p} / \partial {}^R\boldsymbol{r}^T$, respectively.

Let $\boldsymbol{x}$ be a vector of the image features. Assume that the visual target is moving so slowly that one can neglect the velocity of the target comparing to the velocity of the robot. If the feet of the robot are fixed on the ground, we can obtain a velocity relation,

$$ \dot{\boldsymbol{x}} = \boldsymbol{J}_{xp} \, {}^R\dot{\boldsymbol{p}} = \boldsymbol{J}_{xp} \boldsymbol{J}_{pr}^+ \, {}^R\dot{\boldsymbol{r}} = \boldsymbol{J}_{xr} \, {}^R\dot{\boldsymbol{r}}. \tag{4} $$

From eqs.(2) and (4), visual servoing controller, which makes the image feature vector $\boldsymbol{x}$ converge to a given desired trajectory $\boldsymbol{x}_d$ under a control of the feet distance vector $\boldsymbol{l}$ constant to fix the feet on the ground, can be derived as

$$ \begin{aligned} \boldsymbol{u}_r = {} & \boldsymbol{J}_{lr}^+ \boldsymbol{K}_l (\boldsymbol{l}_d - \boldsymbol{l}) \\ & + \left(\boldsymbol{I} - \boldsymbol{J}_{lr}^+ \boldsymbol{J}_{lr} \right) \left\{ \boldsymbol{J}_{xr} \left(\boldsymbol{I} - \boldsymbol{J}_{lr}^+ \boldsymbol{J}_{lr} \right) \right\}^+ \\ & \left\{ \boldsymbol{K}_x (\boldsymbol{x}_d - \boldsymbol{x}) - \boldsymbol{J}_{xr} \boldsymbol{J}_{lr}^+ \boldsymbol{K}_l (\boldsymbol{l}_d - \boldsymbol{l}) \right\}, \end{aligned} \tag{5} $$

where $\boldsymbol{u}_r$, $\boldsymbol{K}_l$ and $\boldsymbol{K}_x$ denote a control input vector and gain matrices, respectively.

In the controller (5), we can obtain the Jacobian matrix $\boldsymbol{J}_{lr}$ from kinematic parameters of the robot. But, since the matrix $\boldsymbol{J}_{xr}$ consists not only of the kinematic parameters that are known, but also of intrinsic and extrinsic camera parameters and of the parameters of the environment, we need to estimate the matrix $\widehat{\boldsymbol{J}}_{xr}$ that satisfies eq.(4) by correcting $\boldsymbol{r}$ and $\boldsymbol{x}$. We utilize a least squares method to identify the non-linear system in the discrete time domain:

$$ \{\widehat{\boldsymbol{j}}_i(k+1) - \widehat{\boldsymbol{j}}_i(k)\} = \frac{\{\boldsymbol{x}(k+1) - \boldsymbol{x}(k) - \widehat{\boldsymbol{J}}_{xr}(k)\boldsymbol{u}_r(k)\}_i}{\rho_i + \boldsymbol{u}_r(k)^T \boldsymbol{W}_{(i,k)} \boldsymbol{u}_r(k)} \boldsymbol{W}_{(i,k)} \boldsymbol{u}_r(k) \tag{6} $$

where $\widehat{\boldsymbol{J}}_{xr}(k)$, $\widehat{\boldsymbol{j}}_i(k)$, $\boldsymbol{u}(k) (= \Delta T \dot{\boldsymbol{r}})$, ρ_i and $\boldsymbol{W}_i(k)$ denote a constant Jacobian matrix, its i-th row vector, a control input vector in the k-th step during sampling interval ΔT, an appropriate positive constant and a weighting matrix, respectively. Using the estimated matrix $\widehat{\boldsymbol{J}}_{xr}$, we can rewrite the controller (5) as

$$ \begin{aligned} \boldsymbol{u}_r = {} & \boldsymbol{J}_{lr}^+ \boldsymbol{K}_l (\boldsymbol{l}_d - \boldsymbol{l}) \\ & + \left(\boldsymbol{I} - \boldsymbol{J}_{lr}^+ \boldsymbol{J}_{lr} \right) \left\{ \widehat{\boldsymbol{J}}_{xr} \left(\boldsymbol{I} - \boldsymbol{J}_{lr}^+ \boldsymbol{J}_{lr} \right) \right\}^+ \\ & \left\{ \boldsymbol{K}_x (\boldsymbol{x}_d - \boldsymbol{x}) - \widehat{\boldsymbol{J}}_{xr} \boldsymbol{J}_{lr}^+ \boldsymbol{K}_l (\boldsymbol{l}_d - \boldsymbol{l}) \right\}. \end{aligned} \tag{7} $$

4 Lifted leg control to increase the body stability

4.1 The body stability and a basic idea

We use a stability margin, which is the shortest distance between the zero moment point (here after, ZMP) and a side of the supporting leg polygon, as a measure of the stability of the legged robot (see Figure 2). If the robot sways the body due to visual servoing, the stability margin becomes small as shown in Figure 2(b). To increase the margin in such a case, it has to lift a leg up and move it, which we call "target leg" in the following.

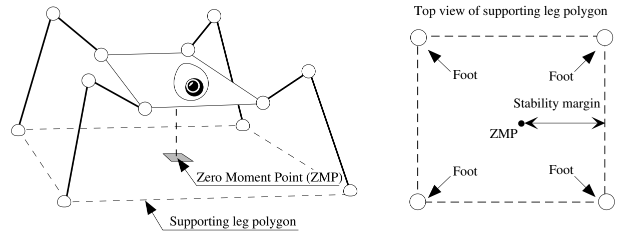

(a) a stable pose

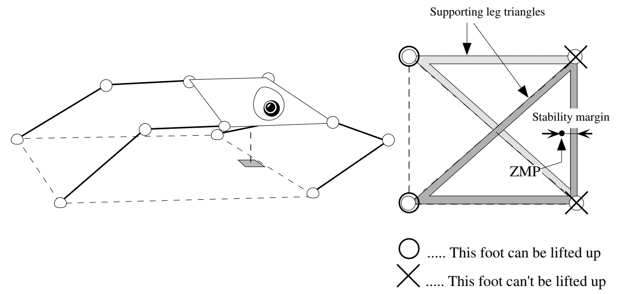

(b) an unstable pose

Figure 2: The relationship between the stability margin and the feet

In Figure 2(b), candidates for the target leg are indicated as "×". They can not be lifted up because ZMP is always inside two supporting leg triangles including the both target legs. In such a case, therefore, the reflective gait control lifts one of the other legs so as to make the target leg to be lifted (see Figure 3(a)), and moves the target leg to increase the stability margin (see Figure 3).

4.2 Lifted leg control algorithm

We can make the reflective gait described above into a simple algorithm as follows. The positions of the lifted legs fall into two cases with respect to the relationship between the supporting legs and v_{zmp}, the velocity of ZMP (see Figure 4): a hind leg case and a fore leg one.

The hind leg case **(The lifted leg is the diagonal leg of leg(A) or leg(B).)** The robot moves the lifted leg to keep ZMP inside the next supporting leg triangle which consists of leg(A) (or leg(B)), leg(C), and the lifted leg. Subsequently, leg(B) (or leg(A)) becomes the lifted leg. (See Figure 4(a).)

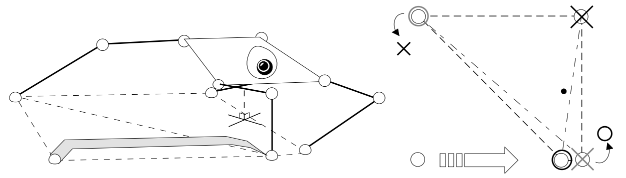

(a) Making the leg a lifted leg

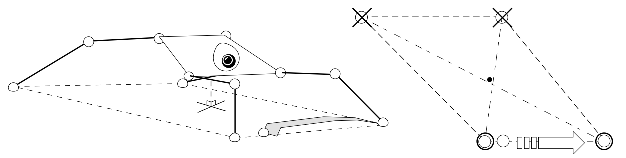

(b) Moving the lifted leg

Figure 3: The reflective gait

The fore leg case **(The lifted leg is the diagonal leg of leg (C).)** The robot moves the lifted leg to appropriate position in front of it, but do not touch down yet. If the ZMP moves into the next supporting leg triangle which consists of leg(A), leg(B), and the lifted leg, then it is naturally touched down, and subsequently leg(C) becomes the lifted leg. (See Figure 4(b).)

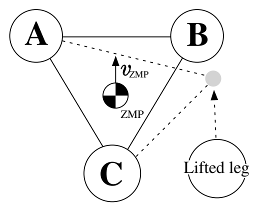

(a) The hind leg case

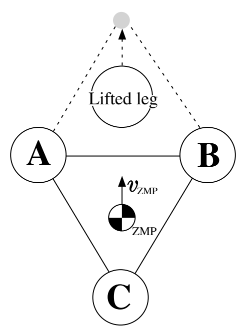

(b) The fore leg case

Figure 4: Supporting leg triangles and a lifted leg

5 The hybrid controller of reflective gait and swaying

We realize a reflective walk by combining the vision-cued swaying control and the lifted leg control. The stance controller utilizes three degrees of freedom (here after, DOFs) and the visual servoing controller uses six DOFs, hence the vision-cued swaying control needs nine DOFs. The lifted leg control also uses three DOFs. Therefore twelve DOFs is necessary/sufficient to realize above two controls in parallel, and we utilize a quadruped robot which has twelve DOFs to implement our proposed method.

We modify the visual servoing controller (7) for four legs as follows.

Let ${}^R\boldsymbol{r}_i$ and l_{ij} denote the i-th foot position vector with respect to Σ_R and a distance between the i-th and the j-th feet, respectively. In order to change the input/output vector of the controller (7) for four legs, we define the stance vector $\boldsymbol{l}$ and the foot position vector ${}^R\boldsymbol{r}$:

$$\boldsymbol{l} = [l_{12}\ l_{13}\ l_{14}\ l_{23}\ l_{24}\ l_{34}]^T \text{ and} \tag{8}$$

$${}^R\boldsymbol{r} = \left[{}^R\boldsymbol{r}_1^T\ {}^R\boldsymbol{r}_2^T\ {}^R\boldsymbol{r}_3^T\ {}^R\boldsymbol{r}_4^T\right]^T. \tag{9}$$

And also we define selection matrices $\boldsymbol{S}_r,\ \boldsymbol{S}_{\bar{r}} \in \Re^{12\times12}$, and $\boldsymbol{S}_l \in \Re^{6\times6}$:

$$\begin{aligned}\boldsymbol{S}_r &= diag[s_1\ s_1\ s_1\ s_2\ s_2\ s_2\ \cdots\ s_4], & (10)\\ \boldsymbol{S}_{\bar{r}} &= diag[\bar{s}_1\ \bar{s}_1\ \bar{s}_1\ \bar{s}_2\ \bar{s}_2\ \bar{s}_2\ \cdots\ \bar{s}_4], \text{and} & (11)\\ \boldsymbol{S}_l &= diag[s_{12}\ s_{13}\ s_{14}\ s_{23}\ s_{24}\ s_{34}], & (12)\end{aligned}$$

where

$$\begin{aligned}s_i &= \text{not}(\delta_{ij}), & (13)\\ \bar{s}_i &= \delta_{ij}, \text{ and} & (14)\\ s_{mn} &= (\delta_{mj})\text{or}(\delta_{nj}) & (15)\end{aligned}$$

$(j\text{: a lifted leg number,}\quad \delta_{ij}\text{: a Kronecker's delta}).$

Then we can obtain following two velocity relations from eqs.(2) and (4):

$$\begin{aligned}\boldsymbol{S}_l\dot{\boldsymbol{l}} &= \boldsymbol{S}_l\boldsymbol{J}_{lr}\ {}^R\dot{\boldsymbol{r}} = \boldsymbol{J}_{slr}\ {}^R\dot{\boldsymbol{r}} \text{ and} & (16)\\ \dot{\boldsymbol{x}} &= \boldsymbol{J}_{xr}\boldsymbol{S}_r\ {}^R\dot{\boldsymbol{r}} = \boldsymbol{J}_{sxr}\ {}^R\dot{\boldsymbol{r}}. & (17)\end{aligned}$$

From eqs.(16) and (17), a visual servoing controller can be derived as

$$\begin{aligned}\boldsymbol{u} = \boldsymbol{J}_{slr}^{+}\boldsymbol{K}_l\boldsymbol{S}_l\left(\boldsymbol{l}_d - \boldsymbol{l}\right) + \left(\boldsymbol{I} - \boldsymbol{J}_{slr}^{+}\boldsymbol{J}_{slr}\right)\\ \left\{\boldsymbol{J}_{sxr}\left(\boldsymbol{I} - \boldsymbol{J}_{slr}^{+}\boldsymbol{J}_{slr}\right)\right\}^{+}\left\{\boldsymbol{K}_x\left(\boldsymbol{x}_d - \boldsymbol{x}\right)\right.\\ \left.-\boldsymbol{J}_{sxr}\boldsymbol{J}_{slr}^{+}\boldsymbol{K}_l\boldsymbol{S}_l\left(\boldsymbol{l}_d - \boldsymbol{l}\right)\right\}.\end{aligned}$$

From eq.(11), a lifted leg controller, which makes the foot position vector ${}^R\boldsymbol{r}$ converge to a given desired trajectory ${}^R\boldsymbol{r}_d$, can be derived as

$$\boldsymbol{u} = \boldsymbol{K}_r\boldsymbol{S}_{\bar{r}}\left({}^R\boldsymbol{r}_d - {}^R\boldsymbol{r}\right), \tag{18}$$

where $\boldsymbol{K}_r$ denote a gain matrix.

6 Experiments

6.1 Experimental systems

In Figure 5, a legged robot TITAN-VIII [6] and its controller used for the experiment are shown. The legged robot is equipped with one camera (EVI-310, SONY). The image from the camera is sent to a tracking unit (TRV-CPD6, Fujitsu) equipped with a high-speed correlation processor [7]. Before starting an experiment, we give three 16[pixel] × 16[pixel] patterns (called reference patterns) to be tracked. During the experiment the unit feeds coordinates where the correlation coefficient is the highest with respect to the reference patterns to the host computer G6-200 (Gateway2000, CPU:Intel Pentium Pro 200MHz) through a PCI-bus link in real-time (33[ms]). Each joint of the legged robot is equipped with a potentiometer to observe its joint angle. Each foot is also equipped with a force sensor to observe its foot force and to estimate the position of ZMP. The observed joint angles and the foot forces are sent to the computer through an A/D converter board (RIF-01, Fujitsu). The computer calculates the desired joint velocities and sends the commands to the velocity controllers of joints through a D/A converter board (RIF-01, Fujitsu). A hand cart is used to move a board on which 3 target marks are drawn.

6.2 Experimental results

We show a result to demonstrate how the proposed method works. At t=2.0[s], the target begins to move rightward at an appropriate speed for the legged robot motion. The robot is initially supported by right-fore-leg(RF), left-fore-leg(LF), and left-hind-leg(LH). The initial lifted leg is right-hind-leg(RH). The robot is swinging its body as the target motion and switches the lifted leg from RH to LF at t=14.0[s]. This is the fore leg case described in section 4.2. Subsequently, it switches the lifted leg from LF to RF (the hind leg case) at t=23.0[s], from RF to LH (the fore leg case) at t=32.0[s], from LH to LF (the hind leg case) at t=39.0[s]. In Figure 6, we can see how the legged robot behaves reflectively to track the visual target.

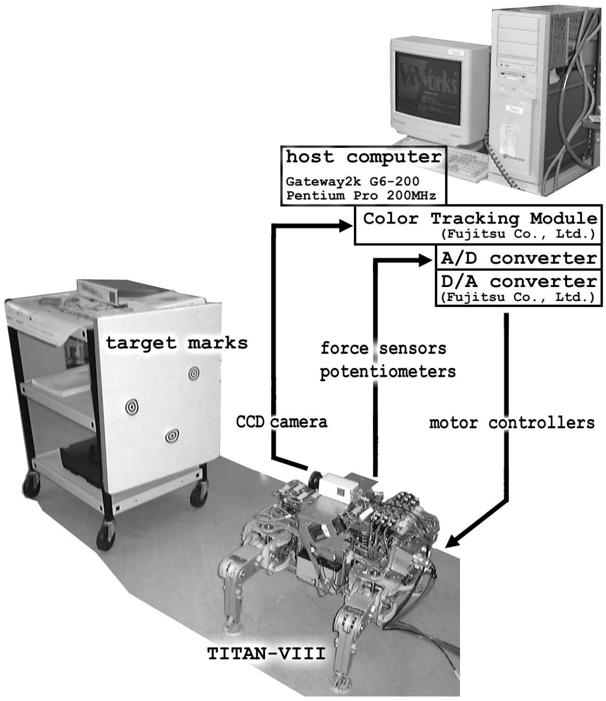

Figure 5: Experimental systems

Error of the position of the target mark 1 (upper left mark in the image plane) is shown in Figure 7. As this graph indicates, the robot can track the target at the first and the second steps.

7 Conclusion

We proposed the reflective walk based on lifted control and vision-cued swaying control, and verified its validity with the preliminary experiments in the real environment. In the experiments, we had two problems that a foot of the lifted leg occasionally bounced off the ground when it touched down, and the robot did not exert a force on the ground due to the extended legs. To solve them, we are examining to utilize simple dynamic characteristics and the manipulating force ellipsoid. In the future work, we will achieve the vision based legged robot navigation by using proposed method.

References

[1] K. Hosoda, T. Miyashita, S. Takeuchi, and M. Asada. Adaptive visual servoing for legged

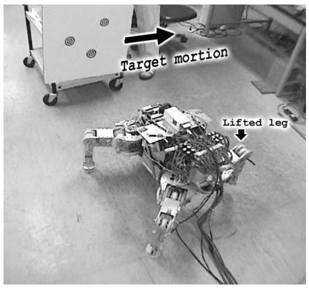

(a) t=2.0[s]

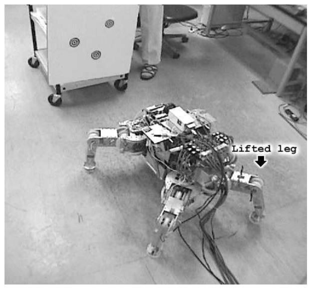

(b) t=9.0[s]

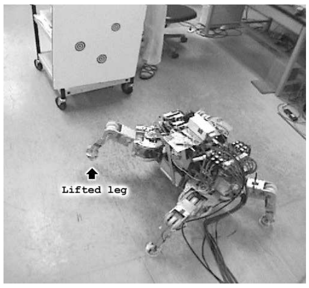

(c) t=14.0[s]

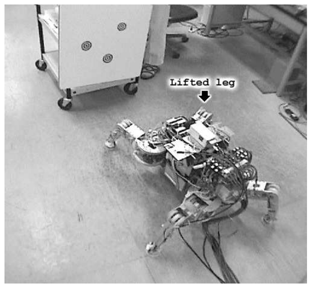

(d) t=23.0[s]

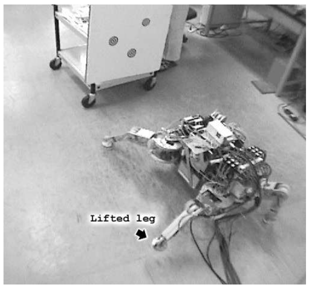

(e) t=32.0[s]

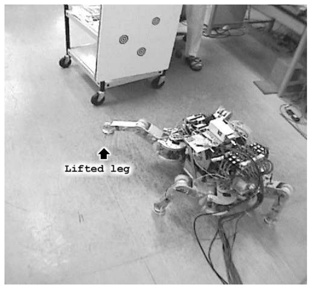

(f) t=39.0[s]

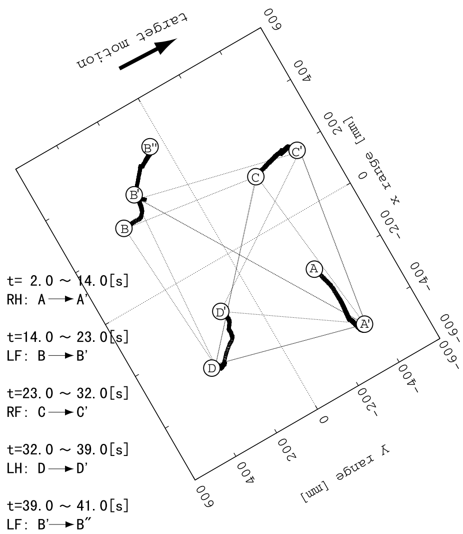

(g) The feet motion w. r. t. a world coordinate frame fixed on the ground

Figure 6: An experimental result: The legged robot walks reflectively.

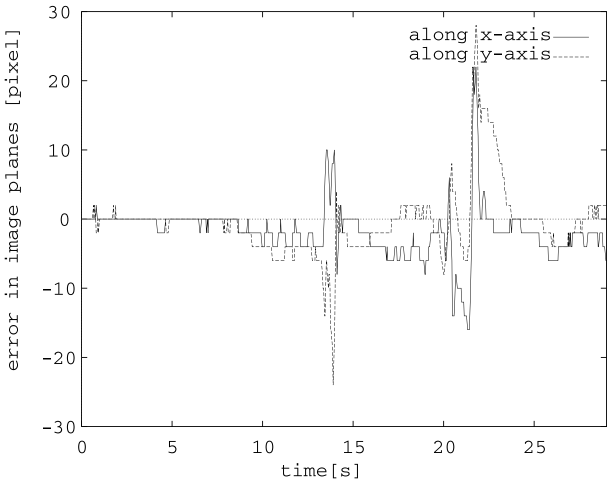

Figure 7: Error of the target mark 1(upper left mark in the image plane)

robots -vision-cued swaying of legged robots in unknown environments-. In *Proc. of the 1997 IEEE/RSJ Int. Conf. on Intelligent Robotics and Systems*, pp. 778–784, 1997.

[2] M. H. Raibert et al. Special issue on legged locomotion. *Int. Journal of Robotics Research*, Vol. 3, No. 2, 1984.

[3] Sami Salmi and Aarne Halme. Implementing and testing a reasoning-based free gait algorithm in the six-legged walking machine, mecant. In *Proc. of International Conference on Intelligent Autonomous Vehicles '95*, pp. ?–?, 1995.

[4] H.Adachi, N. Koyachi, T. Arai, and Y. Shinohara. Human-operated walking control of a quadrupted by event-driven method. In *Proc. of the 1997 IEEE/RSJ Int. Conf. on Intelligent Robotics and Systems*, pp. 260–265, 1997.

[5] K. Hosoda and M. Asada. Versatile visual servoing without knowledge of true jacobian. In *Proc. of the 1994 IEEE/RSJ Int. Conf. on Intelligent Robotics and Systems*, pp. 186–193, 1994.

[6] K. Arikawa and S. Hirose. Development of quadruped walking robot titan-viii. In *Proc. of the 1996 IEEE/RSJ Int. Conf. on Intelligent Robotics and Systems*, pp. 208–214, 1996.

[7] M. Inaba, T. Kamata, and H. Inoue. Rope handling by mobile hand-eye robots. In *Proc. of Int. Conf. on Advanced Robotics*, pp. 121–126, 1993.